



Rapid assessment of gate function and membrane properties of connexin-embedded giant plasma membrane vesicles in the microwell array

Journal:	<i>Analyst</i>
Manuscript ID	AN-ART-01-2025-000036.R1
Article Type:	Paper
Date Submitted by the Author:	27-Jan-2025
Complete List of Authors:	Eguchi, Ryu; University of Hyogo, Isozaki, Yushi; University of Hyogo - Harima Science and Technology Campus, Material Science Suzuki, Masato; University of Hyogo - Harima Science and Technology Campus, Material Science Yasukawa, Tomoyuki; University of Hyogo, Graduate School of Material Science

ARTICLE

Rapid assessment of gate function and membrane properties of connexin-embedded giant plasma membrane vesicles in the microwell array

Received 00th January 20xx,
Accepted 00th January 20xx

DOI: 10.1039/x0xx00000x

Ryu Eguchij,^a Yushi Isozaki,^{a, b} Masato Suzuki^{a, b} and Tomoyuki Yasukawa^{*a, b}

Giant plasma membrane vesicles (GPMVs) incorporating connexin proteins, referred to as connectosomes, serve as promising tools for studying cell membrane properties and intercellular communication. This study aimed to evaluate the membrane capacitance of connectosomes derived from HeLa cells and establish a method for assessing the gate function of connexin hemichannels. We investigated the behavior of dielectrophoresis (DEP) manipulation of connectosomes and HeLa cells by using the microwell array electrodes. The frequency dependence of DEP force for connectosomes and HeLa cells suggested the low membrane capacitance of the connectosomes compared to that of HeLa cells. Positive DEP (p-DEP) was used to trap the connectosomes in microwell array where the relatively strong electric field was formed. This approach facilitated monitoring of fluorescent intensity of individual connectosomes immediately after the solutions were exchanged, enhancing our ability to assess the release dynamics of fluorescence molecules and the hemichannel's open/closed states. The results confirmed that connexin hemichannels were regulated by exterior concentration of Ca^{2+} , allowing selective control over drug storage and release. The method developed in this study elucidates the functional properties of connectosomes and would provide a valuable platform for future applications in targeted drug delivery systems.

Introduction

Giant plasma membrane vesicles (GPMVs) are innovative tools for studying cell membrane properties, as GPMVs can be directly isolated by the chemical treatment of living cells, preserving a significant portion of living cellular components of membrane proteins, lipids and cytoplasm.^{1,2} Since its discovery in the 1970s,³ GPMVs have been used as models for cell membranes in research into mechanical properties^{4,5} and lipid rafts,^{6,7} and its use as a cell mimetic has also been investigated.^{8,9} The principal advantage of GPMVs is that lipid vesicles containing target membrane proteins can be readily obtained from cells with these proteins.¹⁰ For example, the cluster size and density of the calcium channel $\text{Ca}_v1.3$ were quantified by using supported plasma membrane bilayers derived from GPMVs incorporating this protein.¹¹ Furthermore, it has been shown that the extracellular loop of the transmembrane protein Tetraspanin 4 regulates membrane curvature sensitivity by stretching GPMVs with micropipettes and optical tweezers to form lipid nanotubes, taking advantage of the lack of an actin cytoskeleton in GPMVs.¹²

GPMVs with connexin proteins on their membrane are referred to as "connectosomes". Hemichannels (connexons) that are hexamer of connexin proteins formed gap junction

channels by connecting with hemichannels on adjacent cells to provide a transfer of molecules across membranes. The hemichannels permit to be passed molecules below about 1 kDa.¹³ The molecular permeability of hemichannels can also be regulated by the concentration of calcium ions in the vicinity of the connexin protein.^{14,15} Hemichannels remain open at low exterior concentration of Ca^{2+} , while the closed is remained at high. The selective permeability of hemichannels is beneficial for controlling the storage and release of molecules in the connectosomes. Connectosomes have been extensively studied for the use as drug carriers with the ability of selective and direct transport through the gap junctions.¹⁶ The assist by the recognition of receptors expressed on target cells enhanced the selective contact of connectosomes to target cells, resulting in the improvement of the efficiency of drug delivery.¹⁷ Indeed, mutations in connexin proteins have been noted to alter gate function.^{18,19} It is essential to ensure the optimal storage of drugs within the connectosomes under a closed state of hemichannel and the precise release from the connectosomes under an opened state of hemichannel (gate function) for applying connectosomes as effective drug carriers. Therefore, a high-throughput and convenient method for assessing the gate functions of hemichannels is crucial for developing drug carriers used connectosomes. The gate function was typically evaluated by the reduction in fluorescent intensity of fluorescent molecules pre-loaded into the connectosomes following the replacement of the solution with one containing calcium ions by centrifugation.^{16,20} However, the handling of connectosomes in suspensions makes it difficult to monitor the fluorescent intensity from the same connectosomes continuously.

^a Graduate School of Science, University of Hyogo, 3-2-1, Kouto, Kamigori, Aka, Hyogo, 678-1297, Japan. E-mail: yasu@sci.u-hyogo.ac.jp

^b Advanced Medical Engineering Research Institute, University of Hyogo, Hyogo, Japan.

† Electronic supplementary information (ESI) available. See DOI: 10.1039/x0xx00000x

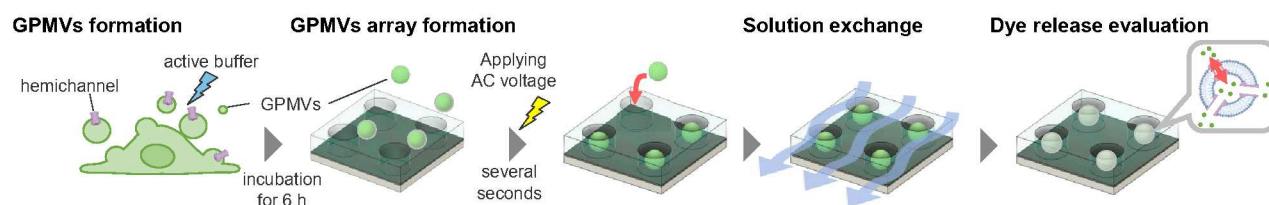


Fig. 1 Schematic for assessing the gate function of connexin hemichannels.

Dielectrophoresis (DEP) is an electrokinetic phenomenon in which dielectrically polarized particles are manipulated in a non-uniform electric field. The DEP method has been successfully applied for the manipulation of a wide range of micro- and nano-materials, including macromolecules (proteins and DNAs), microparticles, cells, microorganisms, liposomes, viruses, and exosomes.²¹ A positive DEP (p-DEP) is an attractive force that directs objects to a strong electric field regions. In contrast, negative-DEP (n-DEP) is a repulsive force that expels objects from the strong electric field regions. The direction of DEP force depends on the applied frequency, the dielectric properties (conductivity and permittivity) of the target materials and the solution in which the materials are dispersed, and the distribution of the electric field. The DEP micromanipulation of cells has been used for cell patterning,^{22–24} cell separation,^{25–27} trapping cells into the microwells for forming cell array,^{28,29} and fabrication of cell aggregation³⁰ and cell pairing.³¹ In particular, the formation of cell arrays in the microwells offers the advantages of robust anchoring of cells and simultaneous observation of multiple cells in the microwells, facilitating rapid solution exchange, and enabling the evaluation of single-cell functions in a time-series manner.

In this study, a simple and rapid method for evaluating the gate function of hemichannels was developed through time-series measurement of the fluorescent intensity emitted from each single connectosome captured in the microwells using p-DEP (Fig. 1). Connectosomes were produced from HeLa cells expressing connexin 43 (Cx43) proteins by chemical treatment. The connectosomes were trapped in the microwells by p-DEP from the arrays of connectosomes. The solution without Ca²⁺ was then injected in the fluidic channel to remain the open state of hemichannels. The fluorescent intensities emitted from each connectosome captured in the microwells were monitored to assess the transfer of fluorescent molecules through hemichannels. The open/closed state of connexin hemichannels was evaluated by estimating the decreased rate of fluorescent intensities. In addition, the membrane capacitance of connectosomes formed by HeLa cells were roughly estimated by the frequency dependences of DEP behavior of connectosomes with transferred hemichannels and HeLa cells.

Experimental

Fabrication of the Microwell Electrode Devices

Microwells (16 μm in diameter, 10 μm in depth) with 10,000 (100 \times 100) array were fabricated by negative photoresist (SU-8

3010, KAYAKU Advanced Materials, Westborough, MA) on an indium tin oxide (ITO) electrode substrate (25 mm square). Distance between centers of the neighboring microwells was set at 32 μm . A 30 μm thick polyester film (Nitto Denko, Osaka, Japan) was used as a spacer to fabricate the fluidic channel (4 mm in width, 7 mm in length) and was sandwiched between the upper ITO electrode substrate (7 mm in width and 20 mm in length) and the lower ITO electrode substrate with the microwell array pattern. The fluidic channels were treated with a 1% (w/v) bovine serum albumin aqueous solution for 24 hours to prevent the nonspecific adsorption of cells and GPMVs.

Cell culture, transfection of expression vector for the connexin proteins, and preparation of connectosomes

HeLa cells were maintained in Dulbecco's modified Eagle medium supplemented with 10% (v/v) fetal bovine serum, 100 U/mL penicillin, and 100 $\mu\text{g}/\text{mL}$ streptomycin and were incubated under humidified conditions containing 5% (v/v) CO₂ at 37 $^{\circ}\text{C}$. HeLa cells (2×10^5 cells/dish) were transfected with the Cx43-mCherry plasmid (Vector Builder Inc., Chicago, IL) using Lipofectamine 3000 (Thermo Fisher Scientific Inc., Waltham, MA) following the procedures provided by the manufacturer. The transfected cells were stained for 30 minutes by immersing in 1 μM 3',6'-Di(*O*-acetyl)-4',5'-bis[*N,N*-bis(carboxymethyl)aminomethyl]fluorescein, tetraacetoxymethyl ester (Calcein-AM, Dojindo Molecular Technologies, Inc., Kumamoto, Japan) 48 hours after transfection. The cells were rinsed twice with a GPMV buffer (10 mM HEPES, 2 mM CaCl₂, 150 mM NaCl, pH 7.4) and then incubated in an active buffer (10 mM HEPES, 2 mM CaCl₂, 150 mM NaCl, 25 mM Paraformaldehyde, 2 mM Dithiothreitol, 125 mM glycine, pH 7.4) for 6 hours to induce the generation of connectosomes.¹⁶ The connectosomes were collected by gentle pipetting in the active buffer, and the resulting solution of dispersed connectosomes was replaced with DEP medium (a mixture of 270 mM sucrose solution and 2 mM CaCl₂ solution, adjusted to be 80 mS m⁻¹ in conductivity) by centrifugation at 17,000 \times g for 20 minutes.

Preparation of liposomes

All lipid molecules used in the preparation of liposomes were obtained from Avanti Polar Lipids Inc. (Alabaster, AL). Liposomes were fabricated by using the gentle hydration method. The lipid solution containing 1,2-Dioleoyl-*sn*-glycero-3-phosphocholine (DOPC), 1,2-Dioleoyl-*sn*-glycero-3-phosphoglycerol (DOPG), 1,2-Dioleoyl-*sn*-glycero-3-phosphoethanolamine-*N*-(lissamine rhodamine B sulfonyl) (Rhodamine-PE), cholesterol, and mannitol were prepared by

dissolving in chloroform/methanol (7:1, v/v). The final concentration of DOPC/DOPG/Rhodamine-PE/cholesterol/mannitol was 0.9:0.1:0.005:0.15:1 in millimolar units. A clean disposable glass vial containing 250 mL of the lipid solution was rotated by hand for 1 minute. A lipid film was formed on the surface of the glass vial by evaporating the organic solvent under blowing nitrogen gas. Then, the vial was kept in vacuo overnight. The dry lipid film was hydrated with 250 mL of 30 mM phosphate buffer solution containing 200 mM sucrose (360 mS m⁻¹ in conductivity) and allowed to stand in a thermostatic incubator at 40°C for a day. The solution with liposomes was replaced with a mixture of 200 mM sucrose and 6.6 mM phosphate buffer (80 mS m⁻¹ in conductivity) by centrifugation at 400 × g for 5 minutes.

DEP manipulation of connectosomes

The device was mounted under an inverted fluorescent microscope (IX73, EVIDENT, Tokyo, Japan) equipped with a CCD camera (DP74, EVIDENT). The connectosome suspension (50 μL) was introduced into the fluidic channel of the device. The AC voltage was applied between the upper and lower ITO electrodes to subject the connectosomes to dielectrophoretic force using the function generator (7075, Hioki E.E. Co., Nagano, Japan). The solution was gently replaced with a Ca²⁺-free buffer (270 mM sucrose and 3 mM MgCl₂, 80 mS m⁻¹ in conductivity) to induce an open state of the hemichannels embedded on the connectosomes captured in microwells. The capture efficiency of connectosomes by p-DEP was defined as the ratio of the number of connectosomes captured in the microwells to the total number of connectosomes in the area under observation with the microscope. The three-dimensional distribution of the electric field strength in the microwell array was calculated by a finite element method solver (COMSOL Multiphysics 5.4, Stockholm, Sweden). A structure containing 9 wells (3 × 3) taking advantage of symmetry conditions was simulated with the element size of "Extremely fine".

Results and discussion

Transfection of connexin protein

The HeLa cells expressing Cx43-mCherry were stained with Calcein-AM. Fig. 2(a) shows images of HeLa cells expressing Cx43-mCherry and GPMVs formed 6 hours after incubating in the active buffer. Almost HeLa cells exhibited green fluorescence by uptaking Calcein-AM to the cytoplasm. However, red fluorescence appeared from approximately 30% of HeLa cells. Many GPMVs were observed around the HeLa cells and emitted red and green fluorescence. The results suggested that Cx43-mCherry and Calcein were successfully transported to the GPMVs from the HeLa cells to form the connectosomes. The collected GPMVs were resuspended in the DEP medium to adjust concentration of 1 × 10⁵ mL⁻¹. Fig. 2(b) shows the fluorescence images of the GPMVs after resuspending in the DEP medium. Four GPMVs in the images exhibited green and red fluorescence indicating that these are connectosomes, while the others exhibited only green. The

ratio of connectosomes with both green and red was about 30% on average, corresponding to the gene transfer efficiency to HeLa cells. Assuming that the formation rate of GPMVs for individual HeLa cells is the same, transfected HeLa cells could produce the connectosomes with connexin. The average diameter of formed connectosomes was estimated and found to be 5.0 μm with the standard deviation of 1.4 (Fig. 2c).

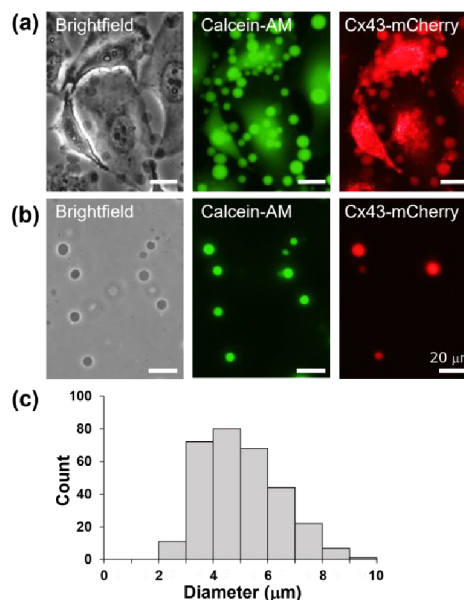


Fig. 2 (a) Optical and fluorescence microscopic images of HeLa cells 6 hours after the incubation in an active buffer. (b) Optical and fluorescence images of isolated connectosomes. (c) Diameter distribution of connectosomes.

Evaluation of dielectrophoretic behavior of connectosomes

The dielectrophoretic behavior of the connectosomes were observed in the microwell electrode device. We focused on connectosomes with diameter of 2-4 μm, although GPMVs with different diameters were manipulated by DEP. This is because DEP behavior depends on the diameter, and the mode of diameter of liposomes prepared to compare DEP behavior was 2-4 μm. Figs. 3(a) and (b) show fluorescence images of connectosomes 90 seconds after AC voltages (5 V_{pp}) with 1 MHz and 3 MHz were applied to both ITO electrodes, respectively. When the AC voltage with 3 MHz was applied, connectosomes moved into the microwells. It is well known that the highest electric field region formed around the bottom of the microwell (Fig. S1). Therefore, p-DEP attracted the connectosomes to the bottom of the microwell. On the other hand, when the AC voltage with 1 MHz was applied, the connectosomes moved to the microwell-to-microwell area where the electric field was the weakest. These results represented that the connectosomes were subjected to the repulsive force derived from n-DEP in this frequency range. Fig. 3(c) shows the ratio of the number of connectosomes trapped in the microwells to the total number of connectosomes in the photos. The ratio of connectosomes in the microwells were below 5% at 1 MHz and increased with an increase of frequency. At a frequency over 2.5 MHz,

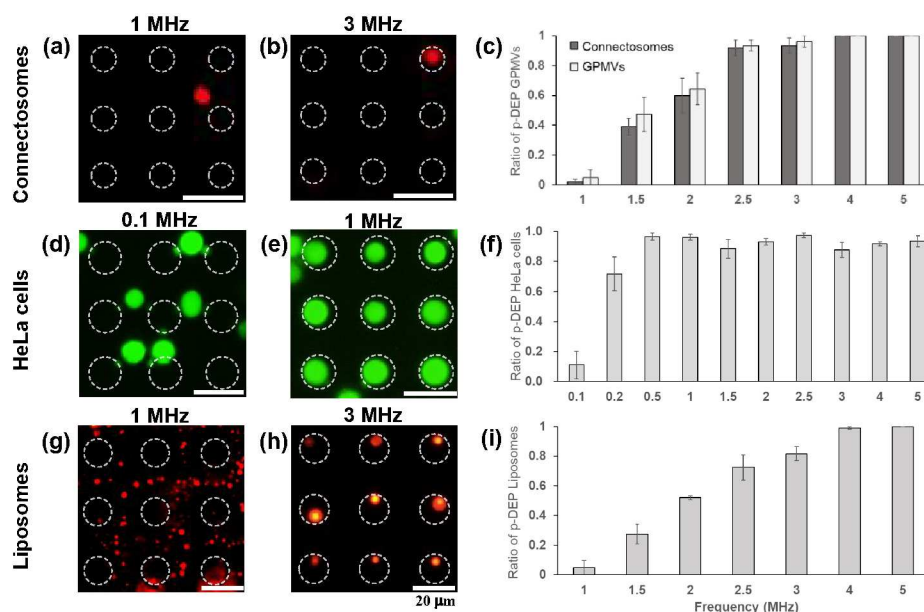


Fig. 3 Fluorescence images 90 seconds after application of (a, e, g) 1 MHz, (b, h) 3 MHz, and (d) 0.1 MHz AC voltages. The white dashed lines indicate the position of the microwells. (c, f, i) Ratio of the number of particles trapped into the microwell at each frequency. Error bars indicate the standard error.

connectosomes were trapped with the ratio over 90%. We defined the frequency with half ratio as a cross-over frequency (f_0). In this definition, the cross-over frequency of the connectosomes was found in the frequency range between 1.5 MHz and 2.0 MHz. The cross-over frequency of GPMVs without connexin was similar to that of connectosomes. These results indicate that the connectosomes and GPMVs have similar membrane capacitances resulting in no significant effect of the presence of connexin proteins on membranes of GPMVs to the dielectric properties, especially the membrane capacitance.

HeLa cells (Figs. 3(d) and (e)) and liposomes (Figs. 3(g) and (h)) also experienced p-DEP in high frequency region to be trapped in microwells. The cross-over frequency of connectosomes was higher than that of HeLa cells that was between 100 kHz and 200 kHz (Fig. 3(f)), and was nearly the same as that of liposomes with a diameter of 3.0 μm (Fig. 3(i)). The experimentally obtained cross-over frequencies of HeLa cells, connectosomes, and liposomes were compared with those calculated based on the theoretical single-shell model of dielectrophoresis (Figs. S2 and S3). The cross-over frequencies can be determined by calculating the frequency dependence of the real part of the Clausius-Mossotti (CM) factors. The real part of the CM factor of the HeLa cells suspended in DEP medium with conductivity (σ_M) of 80 mS m^{-1} and permittivity (ϵ_M) of 78 ϵ_0 (permittivity of vacuum) was calculated by adopting the measured diameter of 15 μm and the following parameters reported previously for a single shell model: membrane capacitance $C_m = 19 \text{ mF m}^{-2}$, cytoplasmic conductivity $\sigma_c = 0.36 \text{ S m}^{-1}$, cytoplasmic permittivity $\epsilon_c = 60 \epsilon_0$, respectively (Table S1). The calculated cross-over frequency of the HeLa cells (120 kHz) was very close to that obtained experimentally.

Moreover, the cross-over frequency of connectosomes was also calculated by using the average diameter of 3.0 μm of the focused connectosomes, and the other electrical parameters

(membrane capacitance, cytoplasmic conductivity, and cytoplasmic permittivity) that were assumed to be the same as those of HeLa cells (Fig. S3). The calculated value (600 kHz) was quite smaller than that obtained experimentally ($f_0 = 1.5\text{--}2.0$ MHz). The membrane capacitance of the connectosomes would be small compared to that of HeLa cells because the DEP spectrum shifts to the high frequency region with the decrease of not only a diameter but a membrane capacitance (Fig. S2). The cross-over frequency of liposomes was also calculated by using the membrane capacitance of 7.5 mF m^{-2} and the diameter of 3.0 μm , that was obtained by the previous report for liposomes composed of DOPC (Fig. S3).³² The calculated value of 1.5 MHz was close to that of the experimental result (between 1.5 and 2 MHz). Thus, the membrane capacitance of connectosomes was presumed to be approximately 7.5 mF m^{-2} , because the electric parameters of interior and exterior and diameter of liposomes were the same as those of connectosomes. In addition, we confirmed that slight high value of interior permittivity for liposomes brought about no significant shift of DEP spectrum.

From these results, we concluded that the membrane capacitance of connectosomes is small compared to that of the parent HeLa cells. The value of membrane capacitance reflects the thickness of the lipid bilayer, permittivity of phospholipid molecules, and surface area per unit area contacting an extracellular solution. The membrane capacitance would most likely reflect the roughness of the membrane since there is no difference in the thickness of the lipid bilayer and the permittivity of phospholipid molecules that make up the membranes of HeLa cells and the liposomes. Therefore, GPMVs containing connectosomes derived from HeLa cells would have smaller membrane roughness than HeLa cells. This membrane flatness would be supported by the fact that there is no

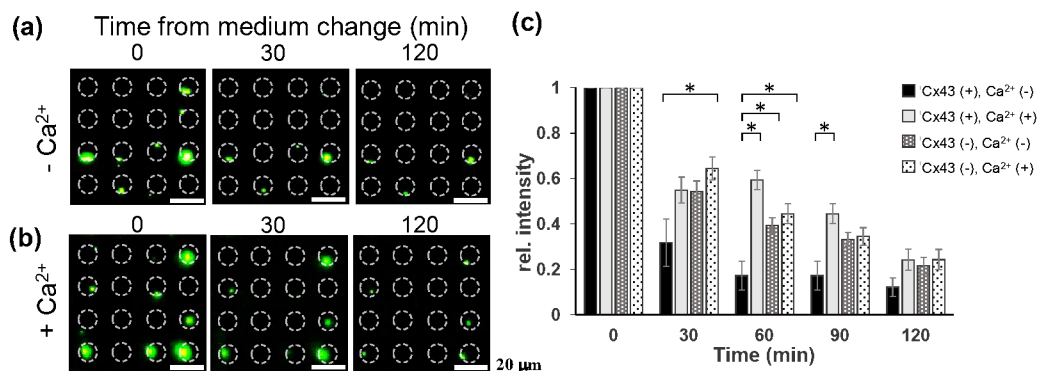


Fig. 4 Fluorescence images of connectosomes trapped in microwells in (a) the absence and (b) presence of Ca²⁺. (c) Time series of relative fluorescence intensity of connectosomes in the absence and presence of Ca²⁺ and connexins. Error bars indicate the standard error. Data were analyzed using Tukey's test. *p < 0.05.

cytoskeletal structure, which defines the shape of membrane and cell, in GPMVs.³³

Evaluation of Connexin Hemichannel Function Using the Connectosomes Array

The gate function of the connectosomes was investigated after the connectosomes suspended in DEP medium with 2 mM Ca²⁺ were trapped in microwells by p-DEP (3 MHz, 5 V_{pp}). Connectosomes were singly trapped in 6% of the wells. This low capture rate is due to the relatively low initial concentration of connectosomes generated by cells cultured on a plane substrate and the low presence ratio of connectosomes (30%) in the total GPMVs. The fluorescent intensity emitted from the Calcein (Mw. 622) encapsulated in the connectosomes was monitored when exchanging the solution to the medium without Ca²⁺ at a flow velocity of approximately 720 μm s⁻¹ (Fig. 4(a)). Due to limitations of the imaging equipment, we analyzed a portion of the connectosomes presented in singles in the wells. The fluorescent intensity of connectosomes decreased to 32% of the initial intensity at 30 minutes after exchanging medium and then continued to decrease to 12% at 120 minutes (Fig. 4(c)). In contrast, in the presence of Ca²⁺, the fluorescence intensity of connectosomes decreased to 55% of the initial intensity after 30 minutes of medium exchange, and to 24% after 120 minutes (Figs. 4(b) and (c)). It is well known that the presence of Ca²⁺ causes the closure of connexin hemichannels, preventing the passage of molecules. Conversely, in the absence of Ca²⁺, connexins undergo a conformational change that causes the opening of connexin hemichannels, allowing passage of molecules.^{14,15,34} Therefore, the rapid decrease in fluorescence intensity of connectosomes in the absence of Ca²⁺ indicated the release of Calcein through the connexin hemichannels. In contrast, GPMVs lacking connexin exhibited a decrease in fluorescent intensity comparable to that observed in connectosomes in the medium containing Ca²⁺ (Figs. 4(c) and S4). The observed decrease in fluorescent intensity would indicate either photobleaching of the Calcein molecule or leakage of Calcein through the lipid membrane that composes GPMVs. Recently, the dye release or uptake through the connectosome membrane have been studied without DEP manipulation. They reported that the membrane permeation

occurred on the similar time scale (1-2 h) in the present work.^{16,20} The results demonstrated that the dielectrophoretic trapping of connectosomes in the microwell facilitated rapid solution exchange. Additionally, the fluorescent intensities emitted from individual GPMVs or connectosomes could be monitored. The monitoring of fluorescent intensities allows for the evaluation of the molecular permeability of individual connectosomes through the hemichannels expressed on the membrane simultaneously.

Conclusions

In this study, we evaluated the characteristics of connectosomes derived from giant plasma membrane vesicles (GPMVs) that incorporate connexin proteins, and established a rapid and efficient method for assessing the gate function of hemichannels. Connectosomes were prepared from HeLa cells through chemical stimulation and confirmed to have an average diameter of 5.0 μm. Using dielectrophoresis (DEP) technology, we observed the behavior of connectosomes, which showed that the trapping efficiency in microwells increased with frequency, achieving over 90% capture at 2.5 MHz.

Furthermore, the membrane capacitance of connectosomes was roughly estimated by comparing the both experimental and calculated cross-over frequencies of connectosomes, HeLa cells, and liposomes and found to be approximately 7.5 mF m⁻². The value estimated for connectosomes was smaller than that of parent HeLa cells.

The fluorescence intensity of calcein encapsulated in connectosomes in the absence of Ca²⁺ rapidly decreased compared to that in the presence of Ca²⁺. This was because the opening of the hemichannels on the membrane in Ca²⁺ free solution allows calcein to permeate through the hemichannels. It is possible to monitor the fluorescence intensities of same connectosomes even after the exchanges of exterior by forming the array of connectosomes trapped in microwells by DEP in the present procedure. Thus, we would rapidly and reliably evaluate the open/closed state of the hemichannels. The precise evaluation of the gate function of connectosomes is crucial for their effective application as drug carriers. Furthermore, the method could be used to evaluate the

permeability (leakage) of lipid bilayers to different fluorescence molecules (fluorescence molecules with different molecular weights, fluorescent proteins, etc.). The method established in this study allows for the time-series tracking of fluorescent intensity from individual connectosomes, providing valuable insights into their functionality.

Author contributions

R. E. conceptualized and planned this work, performed all the experiments and the electric field simulations, and analyzed the data. R. E. wrote the original draft. Y. I., M. S. and T. Y. edited the draft to improve the manuscript. All authors contributed to the discussion of this study and reviewed the manuscript.

Conflicts of interest

There are no conflicts to declare.

Data availability

The data that supports the findings of this study are available in the ESI[†] of this article. The raw data are available on request from the corresponding author.

Acknowledgements

This work was supported by JKA and its promotion funds from AUTORACE to MS, JPNP20004 subsidized by the New Energy and Industrial Technology Development Organization (NEDO) to MS, KSAC-GAP fund from JST to MS, The Futaba research grant program to MS, Terumo Life Science Foundation to MS, and JSPS KAKENHI Grant Numbers 23K26517 to MS and 23K26685 to TY.

References

- 1 E. Sezgin, *Biochim. Biophys. Acta BBA - Biomembr.*, 2022, **1864**, 183857.
- 2 E. K. Fridriksson, P. A. Shipkova, E. D. Sheets, D. Holowka, B. Baird and F. W. McLafferty, *Biochemistry*, 1999, **38**, 8056–8063.
- 3 R. E. Scott, *Science*, 1976, **194**, 743–745.
- 4 D. W. Tank, E. S. Wu and W. W. Webb, *J. Cell Biol.*, 1982, **92**, 207–212.
- 5 J. Steinkühler, E. Sezgin, I. Urbančič, C. Eggeling and R. Dimova, *Commun. Biol.*, 2019, **2**, 337.
- 6 T. Baumgart, A. T. Hammond, P. Sengupta, S. T. Hess, D. A. Holowka, B. A. Baird and W. W. Webb, *Proc. Natl. Acad. Sci.*, 2007, **104**, 3165–3170.
- 7 M. Balakrishnan and A. K. Kenworthy, *J. Am. Chem. Soc.*, 2024, **146**, 1374–1387.
- 8 L. Zartner, M. Garni, I. Craciun, T. Einfalt and C. G. Palivan, *Biomacromolecules*, 2021, **22**, 106–115.
- 9 T. Einfalt, M. Garni, D. Witzigmann, S. Sieber, N. Baltisberger, J. Huwyler, W. Meier and C. G. Palivan, *Adv. Sci.*, 2020, **7**, 1901923.
- 10 C. Zhao, D. J. Busch, C. P. Vershel and J. C. Stachowiak, *Small Weinh. Bergstr. Ger.*, 2016, **12**, 3837–3848.
- 11 N. Schwenzer, N. K. Teiwes, T. Kohl, C. Pohl, M. J. Giller, S. E. Lehnart and C. Steinem, *Commun. Biol.*, 2024, **7**, 1–11.
- 12 R. Dharan, A. Vaknin and R. Sorkin, *Biophys. Rep.*, 2024, **4**, 100149.
- 13 D. A. Goodenough and D. L. Paul, *Cold Spring Harb. Perspect. Biol.*, 2009, **1**, a002576.
- 14 H. Li, T. F. Liu, A. Lazrak, C. Peracchia, G. S. Goldberg, P. D. Lampe and R. G. Johnson, *J. Cell Biol.*, 1996, **134**, 1019–1030.
- 15 W. Lopez, J. Ramachandran, A. Alsamrah, Y. Luo, A. L. Harris and J. E. Contreras, *Proc. Natl. Acad. Sci.*, 2016, **113**, E7986–E7995.
- 16 A. K. Gadok, D. J. Busch, S. Ferrati, B. Li, H. D. C. Smyth and J. C. Stachowiak, *J. Am. Chem. Soc.*, 2016, **138**, 12833–12840.
- 17 A. K. Gadok, C. Zhao, A. I. Meriwether, S. Ferrati, T. G. Rowley, J. Zoldan, H. D. C. Smyth and J. C. Stachowiak, *Biochemistry*, 2018, **57**, 81–90.
- 18 R. Dobrowolski, A. Sommershof and K. Willecke, *J. Membr. Biol.*, 2007, **219**, 9–17.
- 19 D. L. Beahm and J. E. Hall, *Biophys. J.*, 2002, **82**, 2016–2031.
- 20 A. N. Trementozzi, C. Zhao, H. Smyth, Z. Cui and J. C. Stachowiak, *ACS Biomater. Sci. Eng.*, 2022, **8**, 1566–1572.
- 21 P. R. C. Gascoyne and J. Vykoukal, *Electrophoresis*, 2002, **23**, 1973–1983.
- 22 C.-T. Ho, R.-Z. Lin, R.-J. Chen, C.-K. Chin, S.-E. Gong, H.-Y. Chang, H.-L. Peng, L. Hsu, T.-R. Yew, S.-F. Chang and C.-H. Liu, *Lab. Chip*, 2013, **13**, 3578–3587.
- 23 M. Goel, A. Verma and S. Gupta, *Biosens. Bioelectron.*, 2018, **111**, 159–165.
- 24 M. Suzuki, Y. Minakuchi, F. Mizutani and T. Yasukawa, *Biosens. Bioelectron.*, 2021, **175**, 112892.
- 25 H. Song, J. M. Rosano, Y. Wang, C. J. Garson, B. Prabhakarapandian, K. Pant, G. J. Klarmann, A. Perantoni, L. M. Alvarez and E. Lai, *Lab. Chip*, 2015, **15**, 1320–1328.
- 26 Y.-C. Kung, K. R. Niazi and P.-Y. Chiou, *Lab. Chip*, 2021, **21**, 1049–1060.
- 27 T. Yasukawa, J. Yamada, H. Shiku, T. Matsue and M. Suzuki, *Micromachines*, 2020, **11**, 833.
- 28 M. Hata, M. Suzuki and T. Yasukawa, *Biosens. Bioelectron.*, 2022, **209**, 114250.
- 29 S.-M. Yang, Q. Lin, H. Zhang, R. Yin, W. Zhang, M. Zhang and Y. Cui, *Biosens. Bioelectron.*, 2021, **180**, 113148.
- 30 T. Yasukawa, A. Morishima, M. Suzuki, J. Yoshioka, K. Yoshimoto and F. Mizutani, *Anal. Sci.*, 2019, **35**, 895–901.
- 31 Y. Yoshimura, M. Tomita, F. Mizutani and T. Yasukawa, *Anal. Chem.*, 2014, **86**, 6818–6822.
- 32 M. Di Muzio, R. Millan-Solsona, A. Dols-Perez, J. H. Borrell, L. Fumagalli and G. Gomila, *J. Nanobiotechnology*, 2021, **19**, 167.
- 33 F. Schneider, D. Waithe, M. P. Clausen, S. Galiani, T. Koller, G. Ozhan, C. Eggeling and E. Sezgin, *Mol. Biol. Cell*, 2017, **28**, 1507–1518.
- 34 J. Thimm, A. Mechler, H. Lin, S. Rhee and R. Lal, *J. Biol. Chem.*, 2005, **280**, 10646–10654.

1
2
3
4
5
6
7
8
9
10
11
12
13
14
15
16
17
18
19
20
21
22
23
24
25
26
27
28
29
30
31
32
33
34
35
36
37
38
39
40
41
42
43
44
45
46
47
48
49
50
51
52
53
54
55
56
57
58
59
60

Data Availability Statement

The data that supports the findings of this study are available in the ESI of this article. The raw data are available on request from the corresponding author.